

ARTICLE



Activation of RSK2 upregulates SOX8 to promote methotrexate resistance in gestational trophoblastic neoplasia

Shaobin Wu¹, Mingjie Shao¹, Yi Zhang² and Dazun Shi²✉

© The Author(s), under exclusive licence to United States and Canadian Academy of Pathology 2021

Resistance to chemotherapy is frequently driven by aberrantly activated kinases in cancer. Herein, we characterized the global phosphoproteomic alterations associated with methotrexate (MTX) resistance in gestational trophoblastic neoplastic (GTN) cells. A total of 1111 phosphosites on 713 proteins were significantly changed, with highly elevated Ribosomal S6 Kinase 2 (RSK2) phosphorylation (pS227) observed in MTX-resistant GTN cells. Activation of RSK2 promoted cell proliferation and survival after MTX treatment in GTN cell models. Interestingly, RSK2 might play an important role in the regulation of reactive oxygen species (ROS) homeostasis, as manipulation of RSK2 activation affected ROS accumulation and SOX8 expression in GTN cells. In addition, overexpression of SOX8 partly rescued cell proliferation and survival in RSK2-depleted MTX-resistant GTN cells, suggesting that SOX8 might serve as a downstream effector of RSK2 to promote MTX resistance in GTN cells. Highly activated RSK2/SOX8 signaling was observed in MTX-resistant GTN specimens. Further, the RSK2 inhibitor BIX02565 effectively reduced SOX8 expression, induced ROS accumulation, and enhanced MTX-induced cytotoxicity in vitro and in vivo. Collectively, our findings suggested that RSK2 activation could promote MTX resistance via upregulating SOX8 and attenuating MTX-induced ROS in GTN cells, which may help to develop experimental therapeutics to treat MTX-resistant GTN.

Laboratory Investigation (2021) 101:1494–1504; <https://doi.org/10.1038/s41374-021-00651-0>

INTRODUCTION

Gestational trophoblastic neoplasia (GTN) is one of the most successfully treated cancers due to its high sensitivity to chemotherapy¹. Methotrexate (MTX) has been successfully used for the treatment of GTN for decades^{1,2}. However, chemoresistance to MTX still represents a major challenge for GTN treatment. A considerable fraction (20–30%) of low-risk GTN patients fail to achieve complete remission after single-agent MTX treatment³. In addition, about 10–20% of patients with high-risk GTN experience incomplete remission with MTX-containing regimens⁴. Although chemoresistance to MTX in GTN is well recognized, its regulatory mechanisms are not fully understood.

A number of molecular mechanisms responsible for MTX resistance have been documented, including drug efflux via ATP-binding-cassette (ABC) transporters⁵, upregulation of dihydrofolate reductase (DHFR)⁶, involvement of interferon signaling⁷, and redox/reactive oxygen species (ROS) homeostasis⁸. ROS production has been implicated in mediating MTX responses via its effects on downstream cell survival or death signaling cascades. In human ovarian cancer, MTX-induced ROS activated bax/bcl-2-cyt-c release cascading and promoted apoptosis⁸. Recently, accumulating evidence suggested that the reduced ROS level could be the primary reason for MTX resistance in cancer cells. Shen et al. showed that ROS-related mechanisms were involved in cell survival of MTX-resistant choriocarcinoma cells^{9,10}. Our recent proteomics study identified SRY-Box Transcription Factor 8 (SOX8) as a potential regulator of MTX resistance in GTN cells¹¹. SOX8

could reduce drug-induced ROS accumulation through upregulating the expression of antioxidant enzymes Glutathione Peroxidase 1 (GPX1) and Heme Oxygenase 1 (HMOX1) in GTN cells¹¹. However, the molecular mechanisms leading to the upregulation of SOX8 in GTN cells are unclear.

Chemoresistance is frequently driven by aberrantly activated kinase signaling pathways¹². A number of studies indicate that the activation of key protein kinases is intrinsically associated with resistance to anticancer drugs. In leukemia and colorectal cancer, the mitogen-activated protein kinase (MAPK) p38 signaling pathway is closely associated with acquired resistance to cisplatin, irinotecan, and 5-fluorouracil^{13,14}. In gastric cancer, Aurora Kinase B (AURKB) has also been identified as a potential regulator of chemoresistance to cisplatin¹⁵. In addition, over-expression of p21-activated kinase 1 (PAK1) could promote resistance to gemcitabine in pancreatic cancer¹⁶. Therefore, exploring the mechanisms of dysregulated kinase signaling pathways might help identify potential targets to treat drug-resistant cancers.

RSK2 (ribosomal protein S6 kinase, RPS6KA3) is a member of the p90 ribosomal S6 kinase family. RSK2 is regulated under the control of MAPK activities and is positioned upstream of transcription and epigenetic factors involved in cell proliferation, cell transformation, stress-tolerance, and cancer development¹⁷. Although RSK2 has been shown to modulate the sensitivity of ovarian cancer cells to cisplatin¹⁸, its role in the regulation of drug resistance in GTN still remains unknown. In the present study, we identified RSK2 as a potential regulator of MTX resistance in GTN

¹Department of General Surgery, Xiangya Hospital, Central South University, Changsha, China. ²Department of Gynecology, Xiangya Hospital, Central South University, Changsha, China. ✉email: shidzycsu@163.com

Received: 7 February 2021 Revised: 22 July 2021 Accepted: 22 July 2021

Published online: 9 August 2021

cells through a quantitative phosphoproteomics approach. Our findings suggested that RSK2/SOX8 signaling might mechanistically contribute to the development of chemoresistance to MTX in GTN cells, which may improve our understanding of the molecular mechanisms of drug resistance in GTN.

MATERIAL AND METHODS

Reagents and cell lines

Primary antibodies were provided by following sources: p-RSK2 (S227) and β -actin (Affinity Biosciences, Cambridge, MA, USA); RSK2 and SOX8 (Abcam, Danvers, MA, USA). Chemical reagents were provided by following sources: MTX and 2,7-Dichlorodihydrofluorescein diacetate (DCFDA) (Sigma-Aldrich, St. Louis, MO, USA); RSK2 inhibitor BIX02565 (Selleckchem, Houston, TX, USA). Human GTN cell lines JEG3 and JAR were provided by American Type Culture Collection (Manassas, VA, USA). The MTX-resistant sublines JEG3/MTX and JAR/MTX was established as we described previously¹⁹. These GTN cell lines were cultured in Dulbecco's modified Eagle's medium supplemented with 10% fetal bovine serum (Hyclone, Logan, UT), 4 mM glutamine, 100 U/mL penicillin, and 100 μ g/mL streptomycin. Plasmid pCMV3 encoding SOX8 was obtained from Sinobiological Inc (Beijing, China). Lentiviral shRNA plasmids (non-targeting scramble or shRSK2) and Lentiviral plasmids LV242 (empty vector (EV) or FLAG-tagged RSK2 mutants Y707A or S227A) were provided by Genecopoeia (Rockville, MD, USA).

Tandem mass tagging (TMT) labeling and affinity enrichment of phosphopeptides

JAR and its MTX-resistant subline JAR/MTX were used for quantitative phosphoproteomic analysis. Protein extraction, trypsin digestion, and TMT labeling of the peptides were conducted as we described previously¹¹. For affinity enrichment, TMT-labeled peptide mixtures were first incubated with immobilized metal ion affinity chromatography (IMAC) microspheres suspension with vibration in loading buffer (50% acetonitrile/6% trifluoroacetic acid). The IMAC microspheres with enriched phosphopeptides were collected by centrifugation, and the supernatant was removed. To remove nonspecifically adsorbed peptides, the IMAC microspheres were washed with 50% acetonitrile/6% trifluoroacetic acid and 30% acetonitrile/0.1% trifluoroacetic acid, sequentially. To elute the enriched phosphopeptides from the IMAC microspheres, elution buffer containing 10% NH_4OH was added and the enriched phosphopeptides were eluted with vibration. The supernatant containing phosphopeptides was collected and lyophilized for LC-MS/MS analysis.

LC-MS/MS analysis and database search

The phosphopeptides were dissolved in 0.1% formic acid, directly loaded onto a reversed-phase analytical column. phosphopeptides were separated with a gradient from 3 to 17% solvent B (0.1% formic acid in 90% acetonitrile) over 40 min, 17 to 28% solvent B over 12 min, and climbing to 80% in 4 min then holding at 80% for the last 4 min, all at a constant flow rate of 500 nL/min on an EASY-nLC 1000 UPLC system (Thermo Fisher Scientific). The separated phosphopeptides were analyzed in Q ExactiveTM Plus (Thermo Fisher Scientific) with a nano-electrospray ion source. The resulting MS/MS data were processed using MaxQuant search engine (v.1.5.2.8). Tandem mass spectra were searched against the human SwissProt database (20366 entries) concatenated with reverse decoy database. Trypsin/P was specified as cleavage enzyme allowing up to two missing cleavages. The mass tolerance for precursor ions was set as 20 ppm in First search and 5 ppm in Main search, and the mass tolerance for fragment ions was set as 0.02 Da. Phosphorylation on serine, threonine, and tyrosine residues was specified as variable modifications. TMT-6plex quantification was performed. The false discovery rate was adjusted to <1% and minimum score for peptides was set >40.

Cell viability analysis

CCK-8 viability assay was conducted as we described previously¹¹. Briefly, GTN cells were seeded in a 24-well culture plates in triplicate (2×10^4 /well). Cell viability was monitored by CCK-8 viability assay at 48 h after MTX treatment. The optical density (OD) (absorbance) was measured at 450 nm using a Multiskan MK3 microplate reader (Thermo Fisher Scientific, Waltham, MA, USA). IC_{50} values were calculated in SPSS software as described previously¹¹.

Soft agar clonogenesis assay

Soft agar assay was used to examine the in vitro clonogenesis of GTN cells after drug treatment¹¹. Briefly, the 2 mL culture medium with 0.5% agar was first plated into each well of a 6 cm culture dish. After the agar solidified, each well received another 2 mL of 0.35% agar in culture medium containing 1×10^5 cells with or without drugs. After 10–12 days, colonies were fixed by 4% paraformaldehyde and counted.

Bromodeoxyuridine (BrdU) incorporation assay

BrdU incorporation assay was conducted using the Cell Proliferation Assay Kit (Cell Signaling, Boston, MA) as we described previously¹¹. Briefly, GTN cells were plated (4×10^3 cells/well) into 96-well plate and incubated for 16 h before addition of MTX. At 48 h after MTX incubation, cells were labeled with 10 μ M BrdU for 2 h. Cells were then fixed and the DNA was denatured with fixing/denaturing solution. BrdU mouse antibody was added to detect the incorporated BrdU. The absorbance (OD_{450}) was measured using a Multiskan MK3 microplate reader (Thermo Fisher Scientific, Waltham, MA, USA).

Caspase-3 activity assay

Apoptosis of cells after exposure to MTX was detected using the Caspase-3 Colorimetric Assay kit (Abcam) as we described previously¹¹. Briefly, GTN cells (5×10^5 cells) were lysed on ice for 10 min and centrifuged at $10,000 \times g$ for 1 min. Enzyme reactions were carried out on the resulting supernatants in 96-well flat-bottom microplates, using 50 μ l of cell lysate (100 μ g of total protein) for each reaction mixture. The OD (absorbance) was measured at 405 nm using a Multiskan MK3 microplate reader (Thermo Fisher Scientific, Waltham, MA, USA).

Western blotting

Western blot was conducted as we described previously¹¹. Protein lysates (25 μ g) was separated by 10% SDS-PAGE and transferred to Hybond-P PVDF membranes (Amersham Biosciences). Blots were blocked with 5% non-fat dry milk in Tris-buffered saline buffer for 1 h at room temperature and then incubated with diluted antibodies against various proteins for 2 h at room temperature, followed by incubation with horseradish peroxidase-conjugated goat-anti-mouse antibody (Abcam, Cambridge, MA) for 1 h at room temperature. The signal was visualized with an enhanced chemiluminescence detection reagent (Abcam, Cambridge, MA).

KEGG pathway analysis

Kyoto Encyclopedia of Gene and Genome (KEGG) pathway analysis on enriched phosphoproteins was carried out in *Metascape* (<http://metascape.org/gp/index.html>)²⁰. All genes in the genome were used as the enrichment background. More specifically, *P* values are calculated based on accumulative hypergeometric distribution. The most statistically significant term within a cluster is chosen as the one representing the cluster.

Real-time polymerase chain reaction (PCR)

The mRNA level of GPX1 and HMOX1 was measured by Real-time PCR as we described previously¹¹. Briefly, total RNA (1 μ g) was converted to cDNA and then used for SYBR Green PCR. Relative gene expression was determined based on Ct values of GPX1/HMOX1 with reference to β -Actin.

Reactive oxygen species (ROS) measurement

The level of Intracellular ROS was detected by DCFDA fluorescence assay¹¹. GTN cells were incubated with 25 μ M DCFDA for 30 min before ROS measurement. An F97Pro fluorospectrometer (Lengguang Technology, Shanghai, China) was used to measure the DCFDA fluorescence.

Immunohistochemistry (IHC)

Archival paraffin-embedded tissues of patients diagnosed with GTN between 2010 and 2020 were used for IHC analysis. MTX-sensitive GTN ($n = 15$, chemo-naïve patients underwent abdominal surgery/hysterectomy and diagnosed with GTN; these patients achieved complete remission after treated with single-agent MTX or EMACO). MTX-resistant GTN tissues ($n = 23$) were obtained by surgery from patients who developed resistance to single-agent or combined MTX regimens. The research protocols were approved by the research ethics committee in Xiangya Hospital, Central South University (keshen20203665) with informed consent having been obtained from all patients. IHC procedure was conducted as we described

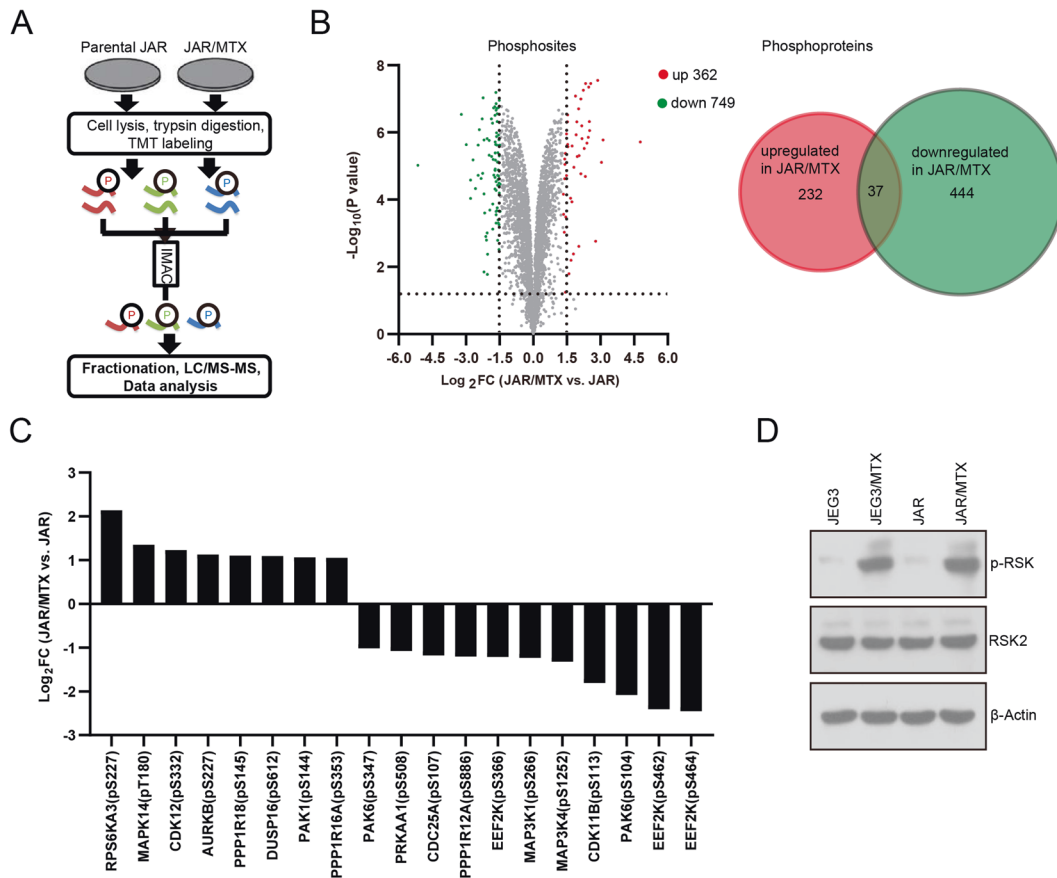


Fig. 1 Quantitative phosphoproteomic analysis on JAR/MTX and JAR cell models. **A** Experimental scheme for the quantitative phosphoproteomic analysis on JAR and JAR/MTX cell models. **B** Differentially expressed phosphosites and phosphoproteins identified by TMT labeling, IMAC enrichment of phosphopeptides, and LC-MS/MS in JAR and JAR/MTX cell models. **C** Altered expression of phosphosites in protein kinases and phosphatases in JAR/MTX cells. **D** Western blotting analysis on p-RSK expression in MTX-resistant GTN sublines.

previously¹¹. Antigen-antibody reactions (Antibody dilution for p-RSK: 1:250; dilution for SOX8: 1:100) were visualized by exposure to 3,3'-diaminobenzidine and hydrogen peroxide chromogen substrate (DAKO, Denmark). The scoring criteria for IHC results are as follows: for staining intensity (Qi), 0 = no staining, 1 = weak staining, 2 = moderate staining, 3 = strong staining; for cell numbers (Qn), 0 = no tumor cells stained, 1 = 5–25% tumor cells stained, 2 = up to 60% tumor cells stained, 3 \geq 60% cells stained. The IHC score is defined as $Q_i \times Q_n$ ²¹.

Animal studies

For xenograft study, JAR/MTX cells (1×10^6) were subcutaneously injected into the left flank of each nude mice ($n = 6$). Inoculated tumors were allowed to establish for 11 days (tumor volume $\sim 50 \text{ mm}^3$) before initiating drug treatments. Phosphate buffered saline (PBS) was used as no treatment control. BIX02565 was orally administered for 7 days (100 mg/kg/day). MTX was administered via intraperitoneal injection for 7 days (2 mg/kg/day). Tumor volume based on caliper measurements was calculated by the modified ellipsoidal formula: tumor volume (mm^3) = $a \times b^2/2$. Mice were sacrificed 19 days after cell inoculation, and the subcutaneous xenografts were removed, washed by PBS, and weighted. The expression of SOX8, Ki-67, and cleaved caspase-3 in xenograft tissues was evaluated by immunohistochemistry. The immunopositivity of cleaved caspase-3 and Ki-67 in each group was calculated in six random, high-power fields.

Statistical analysis

Statistical analysis was conducted using SPSS 16.0 (SPSS Inc, Chicago, IL, USA). Means of two groups were compared by two-tailed unpaired student's *t* test. Differences among more than two groups were analyzed using one-way ANOVA or two-way ANOVA followed by Dunn's multiple comparisons test or Tukey's multiple comparisons test. Spearman rank correlation was used to evaluate the correlation between p-RSK and SOX8 expression. For all the statistical analysis, test with $P < 0.05$ (two-tailed) was considered significant.

RESULTS

Phosphoproteomic profiling of JAR and its MTX-resistant subline JAR/MTX

Quantitative phosphoproteomic analysis was conducted on JAR and JAR/MTX as illustrated in Fig. 1A. Collectively, we detected 9601 unique phosphosites on 3236 proteins, among which 4229 phosphosites were quantifiable in JAR/MTX vs. JAR across all three biological replicates. As shown in Supplementary Fig. 1A, 1B, quantitative phosphoproteomic analysis showed good peptide sequence coverage and peptide distribution. The distribution of phosphosites showed similar pSer:pThr:pTyr ratios (8417:967:217, $\sim 90:10:2$) as previously reported²². Furthermore, according to our criteria ($P < 0.05$, fold change ≥ 1.5 or fold change ≤ 0.67), a total of 1111 phosphosites on 713 proteins were significantly changed in JAR/MTX cells, with 362 upregulated and 749 downregulated (Fig. 1B; Table S1). Upregulated and downregulated phosphosites co-occurred on 37 phosphoproteins (Fig. 1B). KEGG pathway analysis of 713 differentially expressed phosphoproteins was also conducted. KEGG pathways including the *Ribosome*, *Proteoglycans in cancer*, and *Arrhythmogenic right ventricular cardiomyopathy* were highly enriched in the upregulated phosphoproteins (Supplementary Fig. S2). In addition, KEGG pathways including the *Spliceosome*, *RNA transport*, and *mRNA surveillance pathway* were shown to be highly enriched in the downregulated phosphoproteins (Supplementary Fig. S2).

Phosphorylation and dephosphorylation on key phosphosites of protein kinases/phosphatases are crucial for their catalytic activity^{23,24}. Upregulated phosphosites (fold change ≥ 2) including RPS6KA3/RSK2 (pS227), MAPK14/p38 (pT180), CDK12 (pS332),

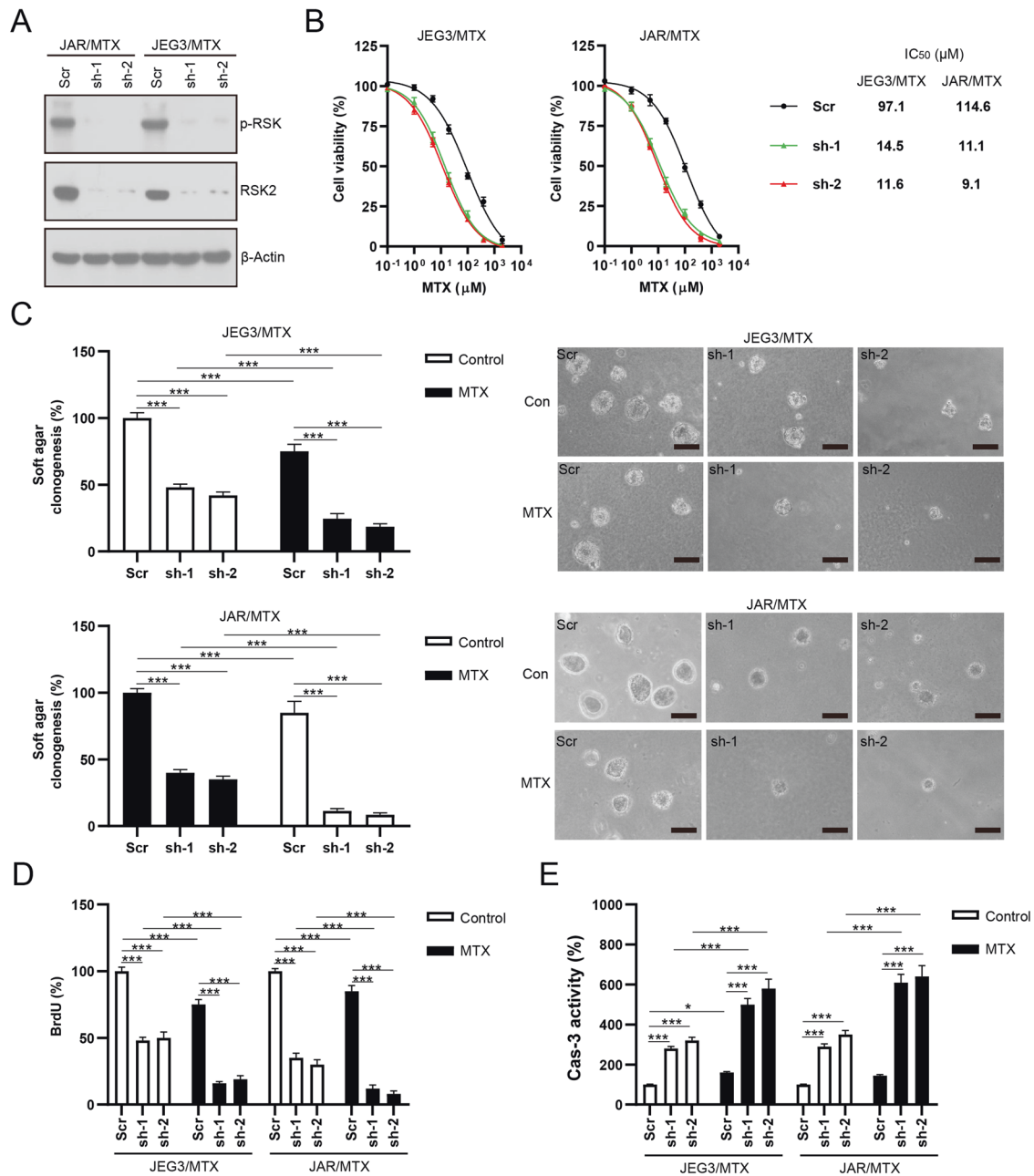


Fig. 2 Knockdown of RSK2 attenuates MTX resistance in MTX-resistant GTN cell lines. **A** RSK2 expression was effectively attenuated by shRNA lentiviruses in JAR/MTX and JEG3/MTX cells. **B** Knockdown of RSK2 increased the chemosensitivity to MTX in JEG3/MTX and JAR/MTX cells. The cell viability in Scr and shRSK2 without MTX treatment was regarded as 100%, respectively. $n = 4$, $***P < 0.001$. **C** Knockdown of RSK2 impaired clonogenesis after MTX treatment (10 μ M) in JEG3/MTX and JAR/MTX cells. Representative micrographs showed the result of soft agar clonogenesis after MTX treatment (10 μ M) in JEG3/MTX and JAR/MTX cells. Bars: 100 μ m. The colony formation in Scr group without MTX treatment was regarded as 100%, respectively. $n = 4$, $***P < 0.001$. **D** Knockdown of RSK2 attenuated the proliferative potential of JEG3/MTX and JAR/MTX cells after MTX treatment (10 μ M) for 48 h. The BrdU incorporation in Scr without MTX treatment was regarded as 100%. $n = 4$, $***P < 0.001$. **E** Knockdown of RSK2 increased caspase-3 activity following MTX treatment (10 μ M) for 48 h in JEG3/MTX and JAR/MTX cells. The caspase-3 activity in Scr group without MTX treatment was regarded as 100%, respectively. $n = 4$, $***P < 0.001$.

AURKB (pS227), and PAK1 (pS144) and downregulated phosphosites (fold change ≤ 0.5) including EEF2K (pS462, pS464), PAK6 (pS104), CDK11B (pS113), CDC25A (pS107), and PRKAA1/AMPK (pS508) were observed in JAR/MTX cells (Fig. 1C). RPS6KA3/RSK2 (pS227) was identified as the top upregulated kinase phosphosite in JAR/MTX cells (Fig. 1C, Supplementary Fig. S3). The highly elevated expression of p-RSK in MTX-resistant GTN sublines was confirmed by western blotting (Fig. 1D). Since RSK2 Ser227 phosphorylation is crucial for its kinase activity²⁵, our findings

imply a function for highly activated RSK2 with MTX resistance in GTN cell lines.

KNOCKDOWN OF RSK2 SENSITIZES MTX-RESISTANT GTN SUBLINES TO MTX TREATMENT

The protein expression of RSK2 and p-RSK was remarkably reduced by RSK2-specific shRNAs, suggesting RSK2 activity was mostly abolished in JAR/MTX and JEG3/MTX cells (Fig. 2A). The

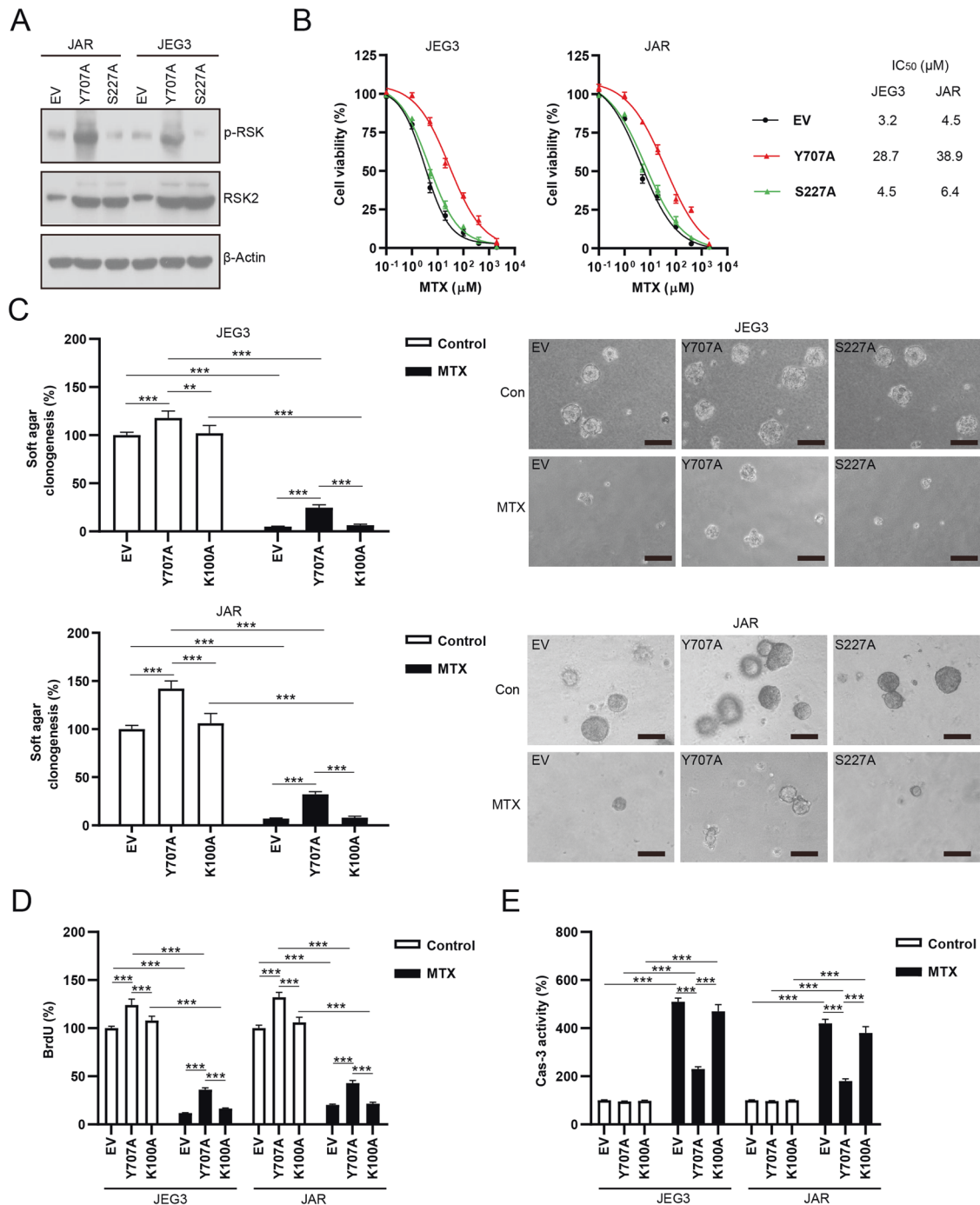


Fig. 3 Over-expression of constitutively activated RSK2 promotes MTX resistance in GTN cell lines. A Overexpression of RSK2 S227A and Y707A mutants in JEG3 and JAR. **B** Over-expression of RSK2 Y707A mutant increased cell viability after MTX treatment in GTN cell lines. **C** Over-expression of RSK2 Y707A mutant rescued soft agar clonogenesis after MTX treatment in GTN cell lines. Representative micrographs showed the result of soft agar clonogenesis after MTX treatment (3 μM) in JEG3 and JAR cells. Bars: 100 μm. The colony formation in EV of each cell line without MTX treatment was regarded as 100%, respectively. $n = 4$, $*P < 0.05$; $***P < 0.001$. **D** Over-expression of RSK2 Y707A mutant enhanced the proliferative potential of GTN cells after MTX treatment (3 μM). The BrdU incorporation in EV of each cell line without MTX treatment was regarded as 100%, respectively. $n = 4$, $**P < 0.01$; $***P < 0.001$. **E** Over-expression of RSK2 Y707A attenuated caspase-3 activity following MTX treatment (3 μM) in GTN cells. The caspase-3 activity in EV of each cell line without MTX treatment was regarded as 100%, respectively. $n = 4$, $***P < 0.001$.

cytotoxic effect of MTX on RSK2-depleted JAR/MTX and JEG3/MTX cells was evaluated by CCK8 assay. RSK2 knockdown increased chemosensitivity to MTX in JAR/MTX and JEG3/MTX cells (Fig. 2B). Soft agar clonogenesis of RSK2-depleted GTN cells was decreased compared to Scr control (Fig. 2C). In addition, RSK2 knockdown further reduced soft agar clonogenesis after MTX treatment

(Fig. 2C). Knockdown of RSK2 also considerably attenuated BrdU incorporation (Fig. 2D). Compared with the Scr group, reduced BrdU incorporation was observed in the shRSK2 group after MTX treatment (Fig. 2D). Further, knockdown of RSK2 also markedly increased caspase-3 activity (Fig. 2E). Compared with the Scr group, increased caspase-3 activity was shown in the shRSK2

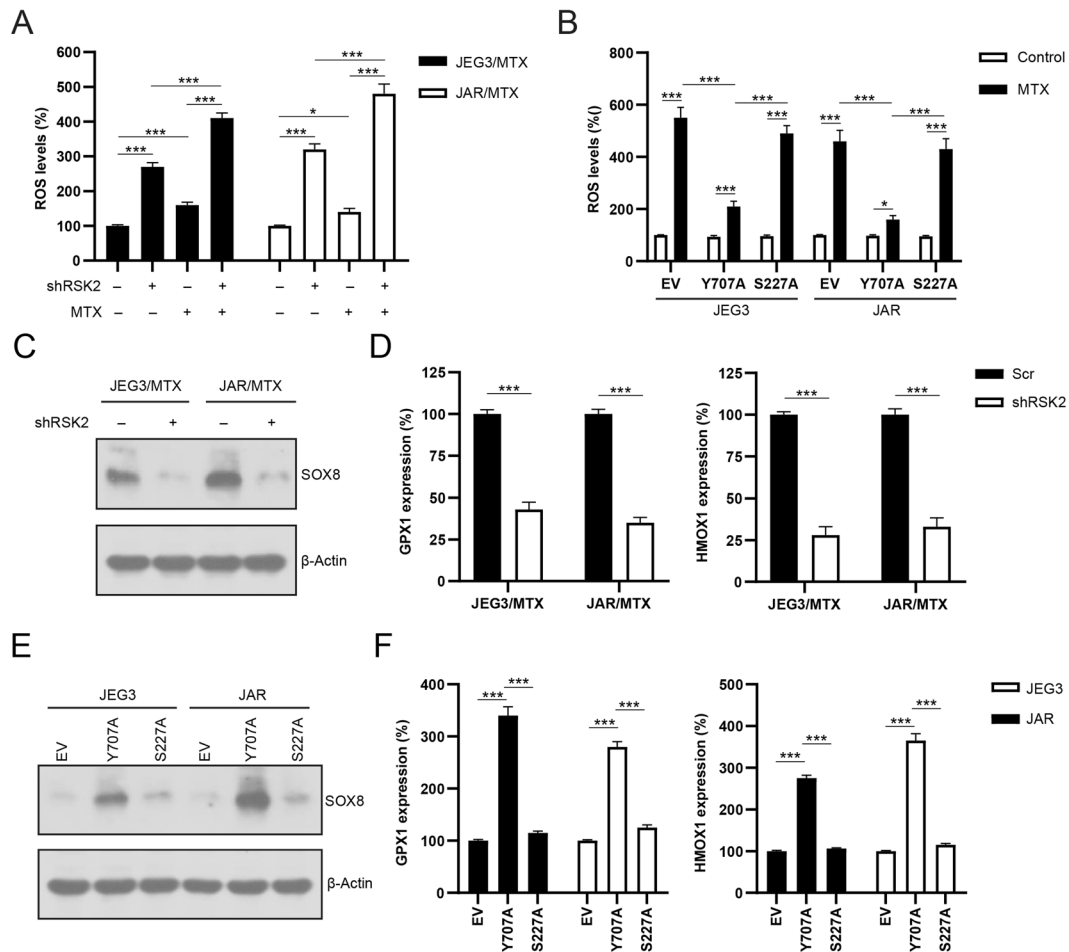


Fig. 4 RSK2 activation reduces ROS generation and induces SOX8 expression in GTN cells. **A** Knockdown of RSK2 enhanced MTX-induced ROS accumulation in JEG3/MTX and JAR/MTX cells. $n = 4$, $***P < 0.001$. **B** RSK2 Y707A mutant attenuated MTX-induced ROS accumulation compared to EV or S227A in JEG3 and JAR cells. $n = 4$, $***P < 0.001$. **C** Knockdown of RSK2 expression reduced the expression of SOX8 in MTX-resistant GTN cells. **D** Knockdown of RSK2 expression significantly reduced the expression of SOX8 downstream genes GPX1 and HMOX1 in MTX-resistant GTN cells. $n = 4$, $***P < 0.001$. **E** Over-expression of RSK2 Y707A mutant increased SOX8 expression in JEG3 and JAR cells. **F** Over-expression of RSK2 Y707A mutant increased the expression of SOX8 downstream genes GPX1 and HMOX1 in JEG3 and JAR cells. $n = 4$, $***P < 0.001$.

group after MTX treatment (Fig. 2E). Therefore, RSK2 plays a critical role in regulating MTX resistance in GTN cells.

Overexpression of constitutively active RSK2 promotes MTX resistance in GTN cells

In order to address the function of activated RSK2 in the regulation of MTX resistance in GTN cells, RSK2 mutants (constitutively active mutant Y707A or kinase inactive mutant S227A²⁶) were expressed in JAR and JEG3 cells. The level of p-RSK was greatly increased only in the Y707A group compared to EV or the S227A mutant (Fig. 3A). The cytotoxic effect of MTX on RSK2 mutant-expressing GTN cells was evaluated by CCK8 assay. A higher IC_{50} value was seen in the Y707A group than in the EV or S227A groups after MTX treatment in JAR and JEG3 cells (Fig. 3B). Although the expression of RSK2 Y707A mutant exhibited a mild effect on soft agar clonogenesis and BrdU incorporation compared with EV or the S227A mutant in JAR and JEG3 cells, it greatly promoted soft agar clonogenesis and enhanced BrdU incorporation after MTX treatment in these cell lines (Fig. 3C, 3D). In addition, less caspase-3 activity was seen in the Y707 mutant group than in the EV or S227A groups after MTX treatment (Fig. 3E). These results suggested that RSK2 activation could promote chemoresistance to MTX in GTN cells.

RSK2 activation reduces ROS generation and induces SOX8 expression in GTN cells

Reduction of MTX-induced ROS contributes to MTX resistance in GTN cells¹¹. However, the role of RSK2 in ROS homeostasis still remains unknown. As shown in Fig. 4A, knockdown of RSK2 induced ROS accumulation in JAR/MTX and JEG3/MTX cells. In addition, a higher ROS level was also observed in the shRSK2 + MTX group compared to the MTX group (Fig. 4A). Further, the RSK2 Y707A mutant greatly attenuated ROS levels compared to EV or the S227A mutant after MTX treatment in GTN cells (Fig. 4B). These findings suggested that RSK2 might promote MTX resistance through reducing MTX-induced ROS accumulation in GTN cells.

Recently, we identified SOX8 as a potential modulator of ROS and drug resistance in GTN cells¹¹. However, whether SOX8 expression is regulated by RSK2 still remains unclear. Our present findings showed that RSK2 knockdown reduced the expression of SOX8 and its downstream antioxidant enzymes GPX1/HMOX1 in JAR/MTX and JEG3/MTX cells (Fig. 4C, 4D). In addition, expression of the RSK2 Y707A mutant increased the expression of SOX8 and its downstream GPX1/HMOX1 compared to EV or the S227A mutant in GTN cells (Fig. 4E, 4F). Therefore, RSK2 might promote MTX resistance through upregulating SOX8 in GTN cells.

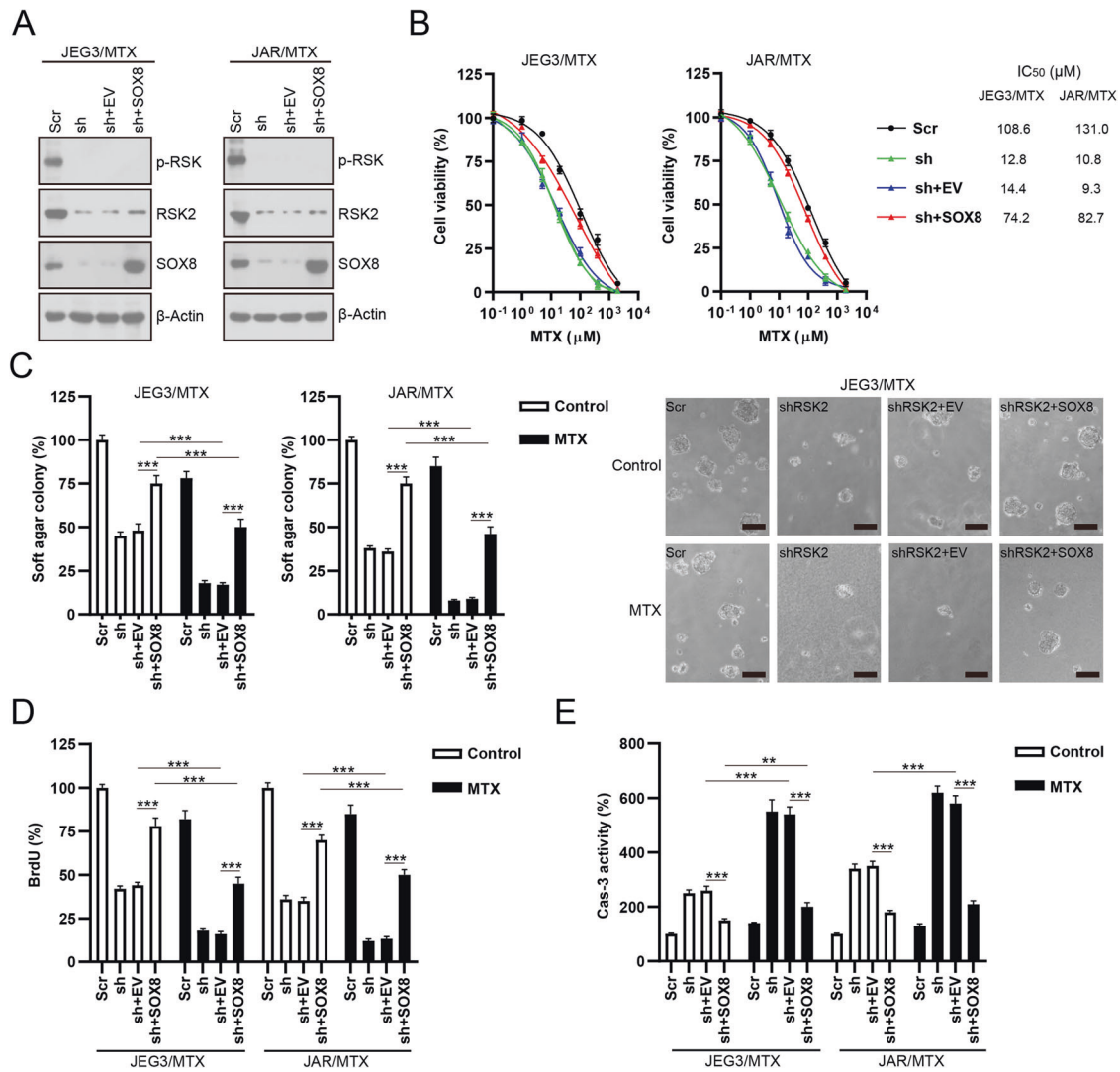


Fig. 5 Over-expression of SOX8 partly rescues the cellular effect of RSK2 knockdown on MTX-resistant GTN cells. **A** Over-expression of SOX8 in RSK2-depleted JEG3/MTX and JAR/MTX cells. **B** SOX8 expression markedly restored the chemoresistance to MTX in RSK2-depleted JEG3/MTX and JAR/MTX cells. **C** SOX8 expression promoted soft agar clonogenesis following MTX treatment in RSK2-depleted JEG3/MTX and JAR/MTX cells. The colony formation in Scr without MTX treatment was regarded as 100%. $n = 4$, $***P < 0.001$. Representative micrographs showed the result of soft agar clonogenesis after MTX treatment (10 μM) in JEG3/MTX cells. Bars: 100 μm. **D** SOX8 expression promoted BrdU incorporation following MTX treatment in RSK2-depleted JEG3/MTX and JAR/MTX cells. The BrdU incorporation in Scr without MTX treatment was regarded as 100%. $n = 4$, $***P < 0.001$. **E** SOX8 expression attenuated caspase-3 activity following MTX treatment in RSK2-depleted JEG3/MTX and JAR/MTX cells. The caspase-3 activity in Scr without MTX treatment was regarded as 100%. $n = 4$, $***P < 0.001$.

Overexpression of SOX8 partly reverses the effect of RSK2 knockdown on MTX-resistant GTN cells

Rescue experiments were conducted in order to confirm the role of SOX8 as a downstream effector of RSK2. SOX8 expression was markedly increased following transfection of a SOX8-expressing plasmid in RSK2-depleted JAR/MTX and JEG3/MTX cells (Fig. 5A). ROS level was effectively attenuated by SOX8 expression in RSK2-depleted JAR/MTX and JEG3/MTX cells (Supplementary Fig. S4A). A higher MTX IC₅₀ was seen in the SOX8 group compared to the EV group in RSK2-depleted JAR/MTX and JEG3/MTX cells (Fig. 5B). Soft agar clonogenesis and BrdU incorporation in the SOX8 group was markedly increased compared with that in the EV group with or without MTX treatment in RSK2-depleted JAR/MTX and JEG3/MTX cells (Fig. 5C, 5D). In addition, Caspase-3 activity induced by RSK2 knockdown was significantly reduced by SOX8 overexpression with or without MTX treatment in RSK2-depleted JAR/MTX and JEG3/MTX cells (Fig. 5E). Therefore, SOX8 might

serve as an important downstream effector of RSK2 in MTX-resistant GTN cells.

RSK2/SOX8 signaling is highly enriched in MTX-resistant GTN tissues

The expression of p-RSK and SOX8 in GTN specimens was evaluated by IHC. The levels of p-RSK and SOX8 were much higher in MTX-resistant GTNs (MTX-R) than in those exhibiting MTX sensitivity (MTX-S) (Fig. 6A, 6B). Highly correlated expression of p-RSK and SOX8 was also observed in these GTN specimens (Fig. 6C). These results highlighted the clinical relevancy of RSK2/SOX8 signaling in MTX-resistant GTNs.

The RSK2 inhibitor BIX02565 potently inactivates RSK2/SOX8 signaling and attenuates MTX resistance in GTN cells

BIX02565, a novel RSK2-specific inhibitor, has been used in a number of cardiovascular studies^{27,28}. Plasma concentrations of

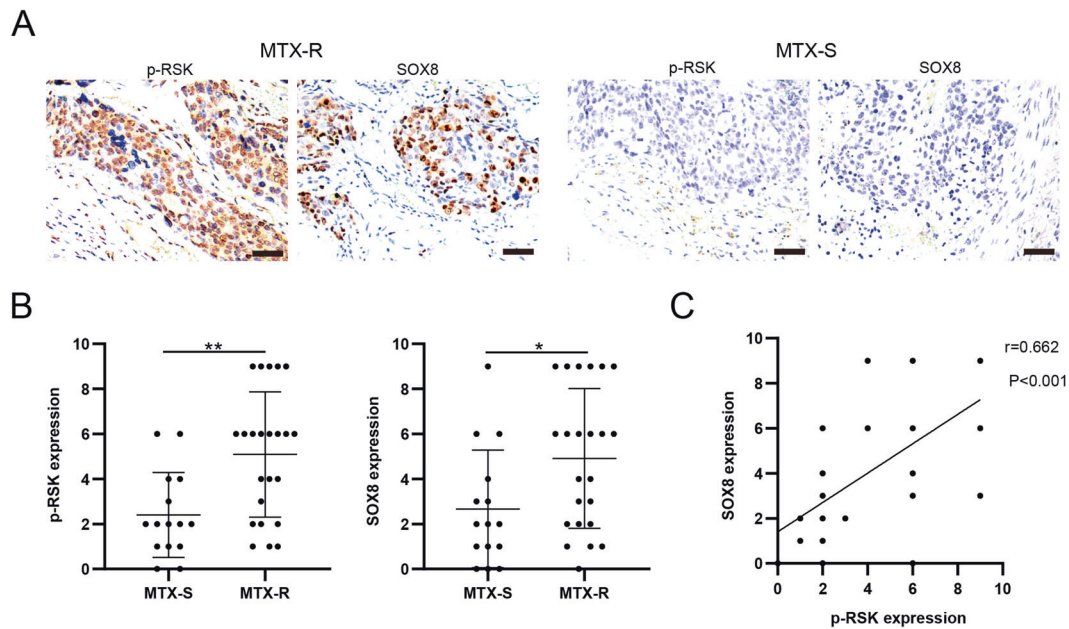


Fig. 6 RSK2/SOX8 signaling was highly enriched in MTX-resistant GTN samples. **A** Immunostaining of p-RSK and SOX8 in GTN samples. Representative IHC staining micrographs were shown for MTX-resistant (left panel) or MTX-sensitive (right panel) GTNs. Bars: 100 μ m. **B** p-RSK and SOX8 were highly expressed in MTX-resistant GTN specimens. * $P < 0.05$; ** $P < 0.01$. **C** High expression of p-RSK was significantly correlated with high expression of SOX8 in GTN specimens.

BIX02565 at $\sim 10 \mu\text{M}$ have been achieved in several animal studies^{27,29}. BIX02565 can potentially inhibit RSK2 kinase activity without affecting PDK1-mediated RSK2 pS227 phosphorylation²⁶. As shown in Fig. 7A, BIX02565 at 5 and 10 μM mostly abolished SOX8 expression in JAR/MTX and JEG3/MTX cells with minimal effects on p-RSK or RSK2 expression. BIX02565 treatment also induced ROS accumulation in a dose-dependent manner in JAR/MTX and JEG3/MTX cells (Fig. 7B). Consistently, higher ROS level was observed in MTX + BIX groups compared to MTX or BIX groups in JAR/MTX and JEG3/MTX cells (Fig. 7C). The cytotoxic effect of BIX02565 on JAR/MTX and JEG3/MTX cells was also evaluated. Co-treatment with BIX02565 increased MTX-induced cytotoxicity compared to MTX or BIX02565 alone in JAR/MTX and JEG3/MTX cells (Fig. 7D). Soft agar clonogenesis of GTN cells treated with BIX02565 was decreased compared to vehicle control (Fig. 7E). In addition, RSK2 inhibition further reduced soft agar clonogenesis after MTX treatment (Fig. 7E). BIX02565 also considerably attenuated BrdU incorporation (Fig. 7F); reduced BrdU incorporation was observed in the BIX02565 group compared to MTX or BIX02565 alone (Fig. 7F). Further, BIX02565 markedly increased caspase-3 activity (Fig. 7G); increased caspase-3 activity was seen in the BIX02565 group compared with MTX or BIX02565 alone after MTX treatment (Fig. 7G). Moreover, we also treated the RSK2-depleted JAR/MTX and JEG3/MTX cells with BIX02565. BIX02565 exhibited minimal effect on the cell viability of RSK2-depleted JAR/MTX and JEG3/MTX cells, suggesting the effect of BIX02565 might be largely attributed to inhibition of RSK2 activity (Supplementary Fig. S4B). Therefore, RSK2 inhibition by BIX02565 could effectively disrupt RSK2/SOX8 signaling and attenuate MTX resistance of GTN cells.

The RSK2 inhibitor BIX02565 suppresses tumor growth and attenuates MTX resistance in a murine xenograft model

The effect of BIX02565 on MTX-resistant GTN cells was evaluated with in vivo experiments. No mice died after BIX02565 treatment (100 mg/kg/day) for 7 days. As depicted in Fig. 8A, BIX02565 alone or BIX02565 + MTX effectively suppressed tumor growth in vivo as compared with PBS control or MTX. The tumor weights in the BIX02565 + MTX group were further reduced compared to the

BIX02565- or MTX-treated groups (Fig. 8B). Hematoxylin/eosin staining revealed severe necrosis within the xenografts following BIX02565 or BIX02565 + MTX treatment as compared with the PBS control or MTX groups (Fig. 8C). BIX02565 or BIX02565 + MTX treatment also reduced SOX8 expression in xenograft tissues (Fig. 8C). Ki-67 positivity was greatly decreased after BIX02565 or BIX02565 + MTX treatment as compared with the PBS group (Fig. 8C, 8D). The combination of BIX02565 with MTX further reduced Ki-67 positivity in JAR/MTX tumors as compared with BIX02565 or MTX alone (Fig. 8C, 8D). In contrast to the PBS group, treatment with BIX02565 or BIX02565 + MTX significantly increased the percentage of cleaved caspase-3-labeled cells in JAR/MTX tumors (Fig. 8C, 8E). BIX02565 + MTX treatment exhibited the highest level of cleaved caspase-3 among the treatment groups (Fig. 8C, 8E). Taken together, these findings confirmed the in vivo efficacy of BIX02565 alone or the BIX02565 + MTX combination for the treatment of MTX-resistant GTN.

DISCUSSION

RSK2 has important functions in cell proliferation, differentiation, transformation, and stress response, despite its function in the regulation of MTX resistance in GTN still remains unknown³⁰. Herein, the identification of RSK2 activation through phosphoproteomics study prompted us to examine the potential role of RSK2 in the regulation of MTX resistance in GTN. Although knockdown of RSK2 greatly attenuated cell proliferation/clonogenesis in MTX-resistant GTN cells, the expression of active RSK2 mutant exhibited a mild effect on cell proliferation/clonogenesis in MTX-sensitive GTN cells. This difference might reflect the differential requirement of RSK2 signaling to maintain cell proliferation in MTX-sensitive and MTX-resistant GTN cells. Our findings also showed that knockdown of RSK2 attenuated MTX resistance in MTX-resistant GTN cells, while constitutively active RSK2 promoted cell survival after MTX treatment in GTN cells. Therefore, RSK2 activation might play a crucial role in the acquisition of MTX resistance in GTN cells.

ROS reduction is a key underlying mechanism of drug resistance in cancer chemotherapy. Shen et al. showed that ROS-neutralizing

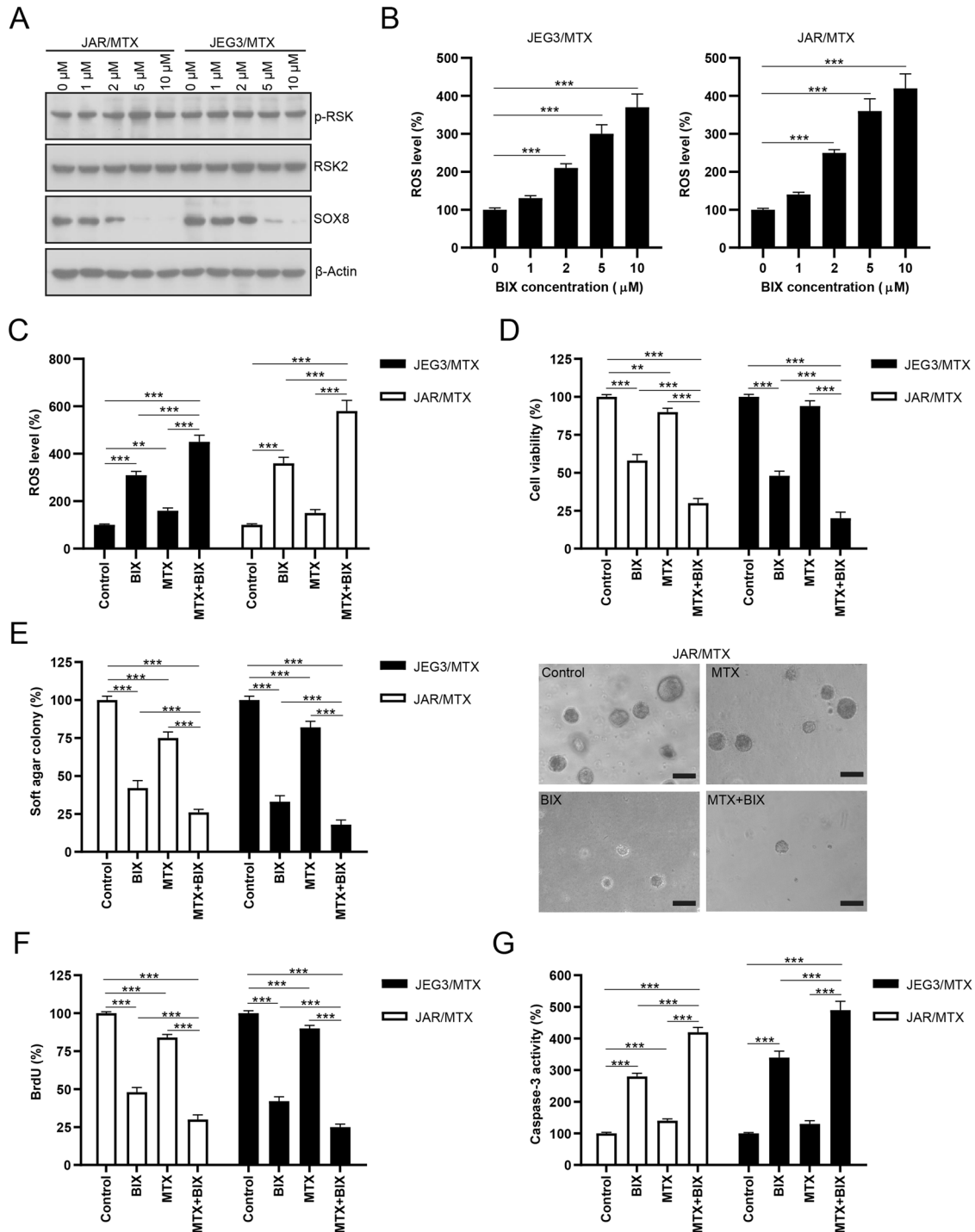


Fig. 7 RSK2 inhibitor BIX02565 downregulates SOX8 expression, induces ROS accumulation, and sensitizes MTX-resistant GTN sublines to MTX. **A** Dose effect of BIX02565 on SOX8 expression in JEG3/MTX and JAR/MTX cells. Cells were treated with vehicle control (DMSO) or indicated doses of BIX02565 for 24 h. **B** Dose effect of BIX02565 on ROS generation in JEG3/MTX and JAR/MTX cells. Cells were treated with vehicle control (DMSO) or indicated doses of BIX02565 for 48 h. $n = 4$, $***P < 0.001$. **C** BIX02565 enhanced MTX-induced ROS generation in JEG3/MTX and JAR/MTX cells. Cells were treated with MTX (10 μM) alone or in combination with BIX02565 (10 μM) for 48 h. The ROS level in vehicle control group was regarded as 100%. $n = 4$, $***P < 0.001$. **D** BIX02565 alone or combined with MTX reduced cell viability in JEG3/MTX and JAR/MTX cells. Cells were treated with BIX02565 alone (10 μM) or in combination with MTX (10 μM) for 48 h. The cell viability in vehicle control was regarded as 100%, respectively. $n = 4$, $***P < 0.001$. **E** BIX02565 alone or combined with MTX impaired clonogenesis in JEG3/MTX and JAR/MTX cells. Cells were treated with BIX02565 alone (10 μM) or in combination with MTX (10 μM) for 12 days. The colony formation in vehicle control (DMSO) was regarded as 100%, respectively. $n = 4$, $***P < 0.001$. Representative micrographs showed the result of soft agar clonogenesis after drug treatment in JAR/MTX cells. Bars: 100 μm . **F** BIX02565 alone or combined with MTX attenuated the proliferative potential of JEG3/MTX and JAR/MTX cells. Cells were treated with BIX02565 alone (10 μM) or in combination with MTX (10 μM) for 48 h. The BrdU incorporation in vehicle control was regarded as 100%. $n = 4$, $***P < 0.001$. **G** BIX02565 alone or combined with MTX increased caspase-3 activity in JEG3/MTX and JAR/MTX cells. Cells were treated with BIX02565 alone (10 μM) or in combination with MTX (10 μM) for 48 h. The caspase-3 activity in vehicle control without MTX treatment was regarded as 100%. $n = 4$, $***P < 0.001$.

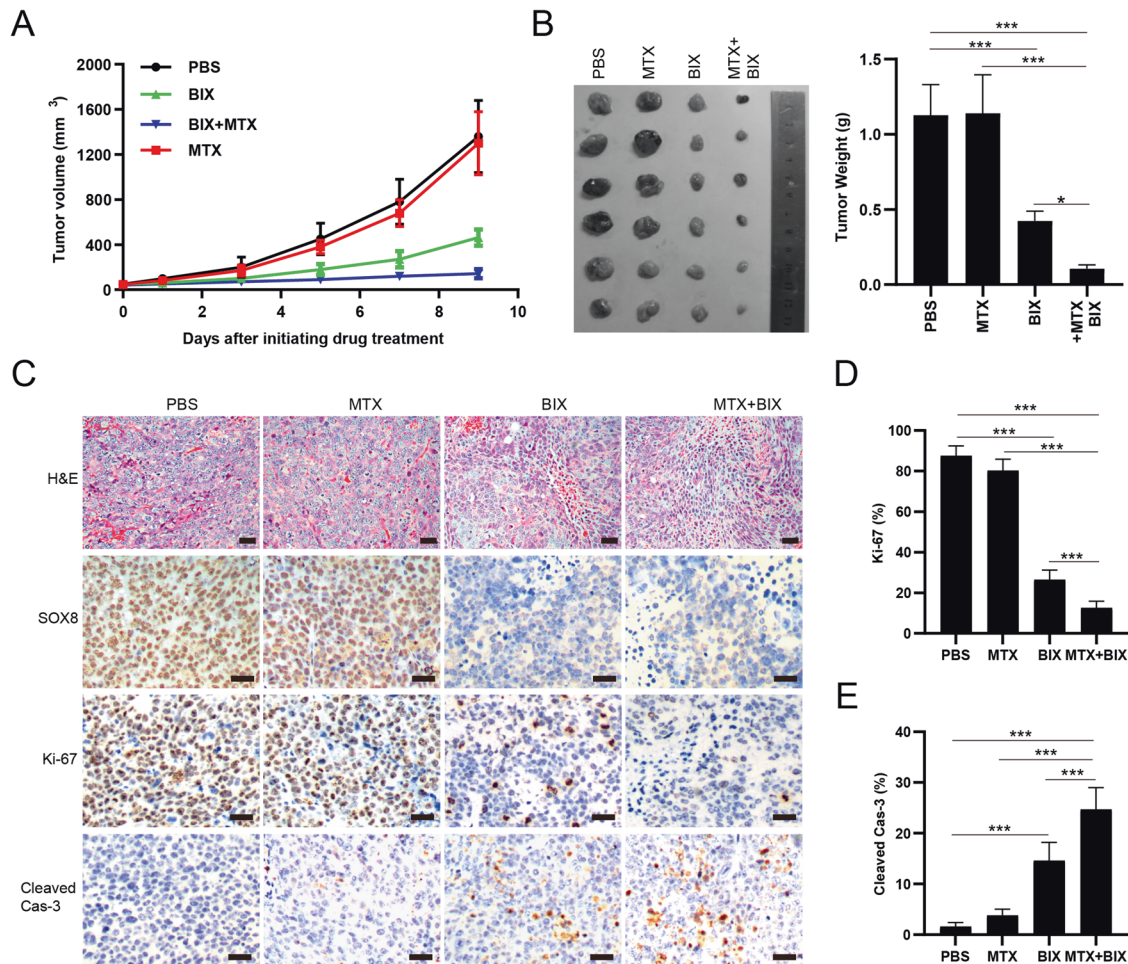


Fig. 8 RSK2 inhibitor BIX02565 reduces SOX8 expression and suppresses tumor growth in JAR/MTX xenograft model. **A** Tumor volume of subcutaneous JAR/MTX xenografts after drug treatment for indicated time. **B** BIX02565 alone or BIX02565 + MTX markedly reduced the weight of JAR/MTX xenografts. $n = 6$, $*P < 0.05$; $***P < 0.001$. **C** IHC staining of the JAR/MTX xenografts after drug treatment. The tissue sections were incubated with primary antibodies (SOX8, Ki-67, and cleaved caspase-3). **D**, **E** Ki-67 and cleaved caspase-3 positivity in drug-treated JAR/MTX xenografts. Bars: 100 μm . $n = 6$, $***P < 0.001$.

mechanisms contribute to cell survival of MTX-resistant choriocarcinoma cells¹⁰. Similarly, our recent study showed that ROS induced by MTX is considerably neutralized in MTX-resistant GTN cells¹¹. However, the effect of RSK2 on ROS homeostasis still remains unclear. In the present study, our findings revealed that RSK2 might exert its pro-survival function by attenuating ROS accumulation in MTX-resistant cells. Consistently, overexpression of a constitutively active RSK2 mutant attenuated MTX-induced ROS in GTN cells. Therefore, RSK2 might modulate MTX resistance via attenuating ROS in MTX-resistant GTN cells.

The transcriptional factor SOX8 plays an important role in cancer development, though its function in the regulation of drug resistance still requires further investigation. Sun et al. showed that SOX8/FOXK1 signaling could promote chemoresistance via suppression of cell senescence and induction of glucose metabolism in ovarian cancer organoids and cells³¹. Similarly, our recent findings showed that SOX8 can promote drug resistance through upregulating antioxidant enzymes (GPX1, HMOX1) and attenuating MTX-induced ROS accumulation in GTN cells¹¹. However, whether SOX8 could serve as a downstream effector of RSK2 to promote MTX resistance in GTN still awaits investigation. Herein, we showed that knockdown of RSK2 or overexpression of a constitutively active RSK2 mutant could regulate the expression of SOX8 and its downstream antioxidant enzymes (GPX1, HMOX1). Impressively, highly activated RSK2/

SOX8 signaling was observed in MTX-resistant GTN samples. Therefore, RSK2 activation might promote cell survival via upregulating SOX8/antioxidant enzymes and attenuating MTX-induced ROS in GTN cells. Our findings also showed that overexpression of SOX8 partly rescued cell survival impaired by RSK2 knockdown in MTX-resistant GTN sublines, suggesting prosurvival signaling pathways other than SOX8 might also be activated by RSK2 and contribute to MTX resistance in GTN cells.

Tremendous efforts have been made to develop small-molecule inhibitors for RSK family kinases. Some RSK2-specific inhibitors, such as BIX02565^{27,29} and FMK³², have been discovered. As a proof of concept, we treated MTX-resistant GTN cells with the RSK2 inhibitor BIX02565 in vitro. Our data suggested that BIX02565 potentially attenuated SOX8 expression, suppressed cell proliferation, and enhanced MTX-induced cytotoxicity in MTX-resistant GTN cell models. The effect of BIX02565 on MTX-resistant GTN cells was also evaluated in a murine xenograft model. BIX02565 treatment effectively reduced SOX8 expression and suppressed in vivo tumor growth. In addition, MTX plus BIX02565 treatment further suppressed tumor growth, decreased Ki67 positivity, and induced apoptosis in vivo. Therefore, our study implies that RSK2 inhibitors are potential agents to treat MTX-resistant GTN, but further investigation is needed in the future.

In conclusion, our findings suggest that RSK2 might promote cell survival by upregulating SOX8 expression and attenuating

ROS accumulation induced by MTX in GTN cells. Further, the RSK2 inhibitor BIX02565 effectively disrupted RSK2/SOX8 signaling and enhanced MTX-induced cytotoxicity in MTX-resistant GTN cells in vitro and in vivo. These findings may have potential clinical value for the development of experimental therapeutics based on RSK2 inhibition to treat MTX-resistant GTN.

DATA AVAILABILITY

The original contributions presented in the study are included in the paper/Supplementary material; further inquiries can be directed to the corresponding author.

REFERENCES

- Braga, A. et al. Challenges in the diagnosis and treatment of gestational trophoblastic neoplasia worldwide. *World J. Clin. Oncol.* **10**, 28–37 (2019).
- May, T., Goldstein, D. P. & Berkowitz, R. S. Current chemotherapeutic management of patients with gestational trophoblastic neoplasia. *Chemother. Res. Pract.* **2011**, 806256 (2011).
- Maesta, I. et al. Effectiveness and toxicity of first-line methotrexate chemotherapy in low-risk postmolar gestational trophoblastic neoplasia: the New England Trophoblastic Disease Center experience. *Gynecol. Oncol.* **148**, 161–167 (2018).
- Bower, M. et al. EMA/CO for high-risk gestational trophoblastic tumors: results from a cohort of 272 patients. *J. Clin. Oncol.* **15**, 2636–2643 (1997).
- Wu, J. & Wang, D. CLIC1 Induces Drug Resistance in Human Choriocarcinoma Through Positive Regulation of MRP1. *Oncol. Res.* **25**, 863–871 (2017).
- Neradil, J., Pavlasova, G. & Veselska, R. New mechanisms for an old drug; DHFR- and non-DHFR-mediated effects of methotrexate in cancer cells. *Klin. Onkol.* **25**, 2587–92587 (2012). **Suppl.**
- Elias, K. M., Harvey, R. A., Hasselblatt, K. T., Seckl, M. J. & Berkowitz, R. S. Type I interferons modulate methotrexate resistance in gestational trophoblastic neoplasia. *Am. J. Reprod. Immunol.* **77** e12666 (2017).
- AlBasher, G. et al. Methotrexate-induced apoptosis in human ovarian adenocarcinoma SKOV-3 cells via ROS-mediated bax/bcl-2-cyt-c release cascading. *Oncotargets Ther.* **12**, 21–30 (2019).
- Zhao, J. et al. AKR1C3 overexpression mediates methotrexate resistance in choriocarcinoma cells. *Int. J. Med. Sci.* **11**, 1089–1097 (2014).
- Shen, Y. et al. The switch from ER stress-induced apoptosis to autophagy via ROS-mediated JNK/p62 signals: a survival mechanism in methotrexate-resistant choriocarcinoma cells. *Exp. Cell Res.* **334**, 207–218 (2015).
- Jun, F., Peng, Z., Zhang, Y. & Shi, D. Quantitative Proteomic Profiling Identifies SOX8 as Novel Regulator of Drug Resistance in Gestational Trophoblastic Neoplasia. *Front. Oncol.* **10**, 557 (2020).
- Yang, W., Freeman, M. R. & Kyprianou, N. Personalization of prostate cancer therapy through phosphoproteomics. *Nat. Rev. Urol.* **15**, 483–497 (2018).
- Grossi, V., Peserico, A., Tezil, T. & Simone, C. p38alpha MAPK pathway: a key factor in colorectal cancer therapy and chemoresistance. *World J. Gastroenterol.* **20**, 9744–9758 (2014).
- Gao, F. & Liu, W. J. Advance in the study on p38 MAPK mediated drug resistance in leukemia. *Eur. Rev. Med. Pharmacol. Sci.* **20**, 1064–1070 (2016).
- Han, X., Zhang, J. J., Han, Z. Q., Zhang, H. B. & Wang, Z. A. Let-7b attenuates cisplatin resistance and tumor growth in gastric cancer by targeting AURKB. *Cancer Gene Ther.* **25**, 300–308 (2018).
- Jagadeeshan, S. et al. P21-activated kinase 1 (Pak1) signaling influences therapeutic outcome in pancreatic cancer. *Ann. Oncol.* **27**, 1546–1556 (2016).
- Cho, Y. Y. RSK2 and its binding partners in cell proliferation, transformation and cancer development. *Arch. Pharm. Res.* **40**, 291–303 (2017).
- van Jaarsveld, M. T. et al. The kinase RSK2 modulates the sensitivity of ovarian cancer cells to cisplatin. *Eur. J. Cancer* **49**, 345–351 (2013).
- Jun, F., Peng, Z., Zhang, Y. & Shi, D. Quantitative proteomic analysis identifies novel regulators of methotrexate resistance in choriocarcinoma. *Gynecol. Oncol.* **157**, 268–279 (2020).
- Tripathi, S. et al. Meta- and Orthogonal Integration of Influenza “OMICS” Data Defines a Role for UBR4 in Virus Budding. *Cell Host Microbe.* **18**, 723–735 (2015).
- Tan, J. et al. PDK1 signaling toward PLK1-MYC activation confers oncogenic transformation, tumor-initiating cell activation, and resistance to mTOR-targeted therapy. *Cancer Discov.* **3**, 1156–1171 (2013).
- Vyse, S. et al. Quantitative phosphoproteomic analysis of acquired cancer drug resistance to pazopanib and dasatinib. *J. Proteom.* **170**, 130–140 (2018).
- Adams, J. A. Activation loop phosphorylation and catalysis in protein kinases: is there functional evidence for the autoinhibitor model? *Biochemistry* **42**, 601–607 (2003).
- Roskoski, R. Jr. Src kinase regulation by phosphorylation and dephosphorylation. *Biochem. Biophys. Res. Commun.* **331**, 1–14 (2005).
- Shimura, Y. et al. RSK2(Ser227) at N-terminal kinase domain is a potential therapeutic target for multiple myeloma. *Mol. Cancer Ther.* **11**, 2600–2609 (2012).
- Somale, D. et al. Activation of RSK by phosphomimetic substitution in the activation loop is prevented by structural constraints. *Sci. Rep.* **10**, 591 (2020).
- Shi, X. et al. The RSK Inhibitor BIX02565 Limits Cardiac Ischemia/Reperfusion Injury. *J. Cardiovasc. Pharmacol. Ther.* **21**, 177–186 (2016).
- Kirrane, T. M. et al. Indole RSK inhibitors. Part 2: optimization of cell potency and kinase selectivity. *Bioorg. Med. Chem. Lett.* **22**, 738–742 (2012).
- Fryer, R. M. et al. Mitigation of off-target adrenergic binding and effects on cardiovascular function in the discovery of novel ribosomal S6 kinase 2 inhibitors. *J. Pharmacol. Exp. Ther.* **340**, 492–500 (2012).
- Lee, C. J. et al. RSK2-induced stress tolerance enhances cell survival signals mediated by inhibition of GSK3beta activity. *Biochem. Biophys. Res. Commun.* **440**, 112–118 (2013).
- Sun, H. et al. Aurora-A/SOX8/FOXK1 signaling axis promotes chemoresistance via suppression of cell senescence and induction of glucose metabolism in ovarian cancer organoids and cells. *Theranostics* **10**, 6928–6945 (2020).
- Kang, S. et al. FGFR3 activates RSK2 to mediate hematopoietic transformation through tyrosine phosphorylation of RSK2 and activation of the MEK/ERK pathway. *Cancer Cell* **12**, 201–214 (2007).

AUTHOR CONTRIBUTIONS

D.Z.S. designed the study; S.B.W., M.J.S. and Y.Z. performed the experiments; S.B.W., M.J.S. and Y.Z. analyzed the data; D.Z.S. wrote the paper. All authors have read and approved the final version of the paper.

FUNDING

This work was supported by The Science and Medicine Joint Project of Hunan Province (Grant Number: 2019JJ80013); National Natural Science Foundation of China (Grant Number: 82000585).

COMPETING INTERESTS

The authors declare no competing interests.

ETHICS APPROVAL

The studies involving human participants were reviewed and approved by the Institutional Review Board in Xiangya Hospital, Central South University (keshen20203665). The patients/participants provided their written informed consent to participate in this study. The animal study was reviewed and approved by the Institutional Animal Care and Use Committee in Xiangya Hospital, Central South University (dongwulunshen20203665).

ADDITIONAL INFORMATION

Supplementary information The online version contains supplementary material available at <https://doi.org/10.1038/s41374-021-00651-0>.

Correspondence and requests for materials should be addressed to D.S.

Reprints and permission information is available at <http://www.nature.com/reprints>

Publisher's note Springer Nature remains neutral with regard to jurisdictional claims in published maps and institutional affiliations.